EVALUATION OF A SOLAR POWERED DISTILLATION UNIT AS A MITIGATION TO WATER SCARCITY AND CLIMATE CHANGE

M.C. Georgiou[*,1], A.M. Bonanos[1], J.G. Georgiadis[1,2]

[1] *Energy Environment and Water Research Center, The Cyprus Institute, Nicosia 2121, Cyprus*
[2] *Department of Mechanical Engineering, University of Illinois at Urbana-Champaign, Urbana Il, 61820, USA*

Abstract

Cyprus, an island facing water scarcity periods throughout its history, has to cope with even more intense periods due to climate change as it is predicted by several climate models. The aim of the present study is to evaluate the performance of a single effect distillation unit and the potential of its integration with a concentrated solar power system as a mitigation technique to the water scarcity.

Specifically, a single effect distillation unit for seawater desalination was developed and its performance in terms of performance ratio (ratio of distillate product and steam fed to the unit) was experimentally investigated. The main parameters examined were the thermal input power and the temperature and flowrate of the inlet seawater. For several seawater flow rates, three different initial heat loads were used ($T_{st,1}$, $T_{st,2}$, $T_{st,3}$). Experiments were repeated for two seawater inlet temperatures, T_{sw1}, T_{sw2}. A one-dimensional model based on conservation of mass and energy was developed to predict the performance of the device.

The results showed that lower heat input load results to a higher value of the performance ratio of the unit and also under constant heat load, a higher temperature of the seawater lead to higher distillate product. The developed model adequately captured the behavior of the device. Thus, it is concluded that such a unit should be expanded into a multiple-effect unit and also implemented with a concentrated solar power system as a mitigation technique to the water scarcity of the island.

Keywords: Multiple-Effect distillation, desalination, solar thermal energy, performance ratio, CSP

Nomenclature

Symbols

Cp	*specific heat capacity*
m	*mass flow-rate*
PR	*performance ratio*
Q	*thermal load*
T	*temperature*
U	*heat transfer coefficient*
X	*salinity*
λ	*latent heat of vaporization*

Subscripts

b	*brine*
cw	*cooling water*
d	*distillate*
e	*evaporator*
st	*steam*
sw	*seawater*
v	*vapour*

[*] Presenting author: email: m.c.georgiou@cyi.ac.cy, Tel : (+357) 22 208 604, Fax: (+357) 22 208 625

1. Introduction

1.1 Water situation in Cyprus

Cyprus throughout its history has been facing several periods of water scarcity due to a combination of limited availability and excess demand of water [1]. According to the Water Exploitation Index, an index that compares available water resources in a country to the amount of water used, presented in Fig. 1 for several European countries, Cyprus is considered to be water stressed. An index above 20% indicates water poverty for an EU country and Cyprus had an index above 40% in 2007 [2].

The two main water-consuming sectors in the country are agriculture and households. Cyprus has already faced severe droughts and water scarcity with the most recent one being in 2008, where it had to import water from Greece to satisfy drinking water demand and to enforce restrictions on household supply [3].

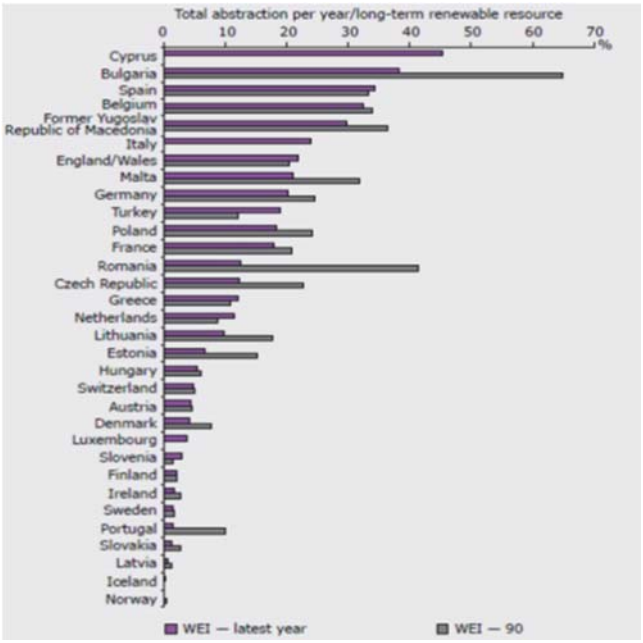

Fig. 1 Water Exploitation Index (WEI) [4].

According to the Intergovernmental Panel on Climate Change (IPCC), climate change is defined as a change in the state of the climate that can be empirically identified. This change can be identified by changes in the mean and/or the variability of climate properties and it is lengthened for an extended period, typically decades or longer. Whether this change is caused by human activity or due to natural variability, a climate change term refers to any change in climate over time [5].

Europe and especially the Eastern Mediterranean region is expected to be affected by climate change. Projections according to the IPCC SRES scenario A2 predict that there will be an increase in both minimum and maximum temperatures by about 3 °C in the mid-21st century and by more than 4 °C by the end of the century. The projected impacts on temperature estimated for 2071-2100 relative to the baseline period of 1961-1990 are shown in Fig. 2(a).

The temperature increase observed in Europe has a direct effect in the atmosphere. Within a warmer atmosphere more water vapour is contained therefore the precipitation rate is also directly affected. Rainfall is a regional phenomenon that differs strongly from region to region. Thus, while in northern Europe rainfall and snowfall have increased, in southern Europe droughts are more frequently observed, as shown in Fig. 2(b).

Annual precipitation levels are forecasted to decline by 15-25% over the same period [6]. The Mediterranean is very likely to face continuous droughts and hence suffer from increasing water scarcity, declining crop yield and increasing desertification. Water availability may be reduced by as much as 20-30% under a 2 °C increase global warming scenario or 40-50% under a 4 °C warming scenario.

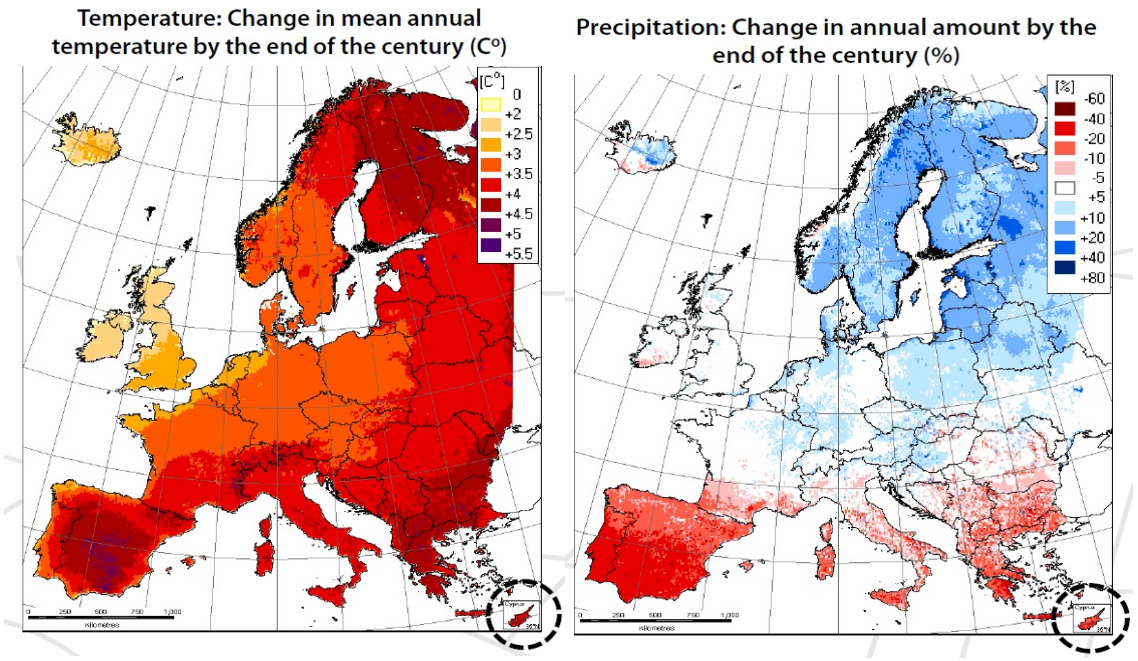

Fig. 2: (a) shows the predicted change in mean annual temperature by the end of the century, while (b) shows the predicted change in annual amount of precipitation by the end of the century [7].

1.2 Seawater desalination as a mitigation technique – Multiple Effect Distillation

As a result of water scarcity, alternate means for obtaining freshwater, such as through seawater desalination [8], must be pursued. Further, the increasing demand for freshwater, due to population increase, coupled with the decreased rate of replenishment of the freshwater resources due to climate change impacts, necessitates the pursuit of desalination through renewable energy technologies.

A desalination process separates saline water into two parts - one that has a low concentration of salt (treated water or product water), and the other with a much higher concentration than the original feed water, usually referred to as brine concentrate or simply as brine. Commercially, the major types of technologies used for desalination can be divided in two types: thermal desalting technology and membrane desalting technology. Thermal desalting technologies include Multi-Stage Flash distillation (MSF), Multi-Effect Distillation (MED) and Vapor Compression (VC), while membrane technology includes Electro Dialysis (ED) and reverse osmosis (RO).

As the name implies, thermal technologies involve the heating of saline water and collecting the condensed vapour (distillate) to produce pure water. The MED process has been used since the late 1950's and early 1960's and consists of several consecutive vessels (effects), maintained at decreasing levels of pressure (and temperature), leading from the first (hot) stage to the last one (cold). The main advantage of an MED unit compared to RO is lower electricity consumption due to the higher thermal input needs. Thus the electrical energy for RO is about 3.5-4 (kWh/m^3) while for MED unit is about 1-2 (kWh/m^3). Compared to other thermal technologies such as MSF, MED has less total primary energy demands, lower power consumption and also has a higher performance ratio. Additionally the usage of Plate Heat Exchangers (PHE) resulted in higher heat transfer coefficients and also lower fouling resistances [9].

Each effect contains a multiphase heat exchanger. Seawater is introduced in the evaporator side and heating steam in the condenser side. As the seawater flows down the evaporator surface, part of it is evaporated, while the remainder collects at the bottom of each effect as brine [10]. The pure water vapour raised by seawater evaporation at a lower temperature than the vapour in the condenser, due to the boiling point elevation observed in saline solutions. However, it can still be used as heating medium for the next effect where the process is repeated [11].

The decreasing pressure from one effect to the next one allows brine and distillate to be drawn to the next effect where they will flash and release additional amounts of vapour at the lower pressure [12]. This additional vapour will condense into distillate inside the next effect. In the last effect, the produced steam condenses on a heat exchanger, called distillate or final condenser, and which is cooled by the seawater used in the first effect.

1.3 Seawater desalination powered by solar thermal energy

The main drawback of all seawater desalination technologies, however, remains the high energy consumption. In Cyprus it has been estimated that the production of 1 million m^3/day fresh water requires 10 million tons of oil per year [13]. Due to high cost of conventional energy sources and considering the increasing trend in fossil fuel prices, renewable energy sources have gained more attention since their use in desalination plants will save convectional energy for other applications, reduce environmental pollution and provide free, renewable energy source [14]

As with any technology that generates power through prior heat generation, concentrated solar power (CSP) has scope for the application of co-generation. CSP plants can generate electricity which can subsequently be used for membrane desalination via reverse osmosis, but they can also produce combined heat and power [15-16].Thus, also thermal desalination methods like MED can be coupled to a CSP plant in an integrated co-generation scheme, as schematically depicted in Fig. 3. The thermodynamic integration of the electricity and desalination cycles, allows for increased efficiency to be achieved in both cycles, due to the larger fraction of useful energy extracted from each unit of thermal energy introduced to the system [**Error! Reference source not found.**17-18].

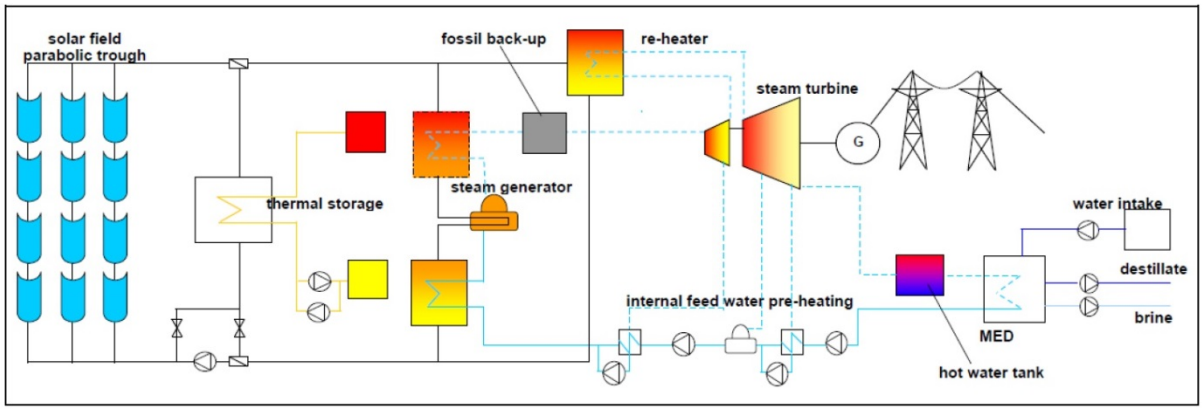

Fig. 3 Multi-Effect Desalination Using Heat and Power from a CSP Plant [19].

One application in which heat from CSP plants could be used is desalination, especially at a time when many regions, such as the Middle East and Northern Africa (MENA) region, that are suitable for CSP due their large levels of solar irradiation, face severe fresh water deficits. MED is more efficient than MSF in terms of primary energy and electricity consumption and has a lower cost. Moreover, the operating temperature of MED is lower, thus requiring steam at lower pressure if connected for combined generation to a steam cycle power plant. Thus, the combination of CSP with MED, as it is shown in Fig. 3 will be more effective than a combination of CSP and MSF desalination.

In the present paper, a single-effect distillation (MED) unit for seawater desalination was constructed in order to experimentally characterize its performance when operating under variable thermal load or under variable seawater feed flowrates. This allows the optimal operating conditions to be determined, particularly under low-flow conditions. A one-dimensional theoretical model to predict the performance of the device is developed and validated against the experimental results obtained.

2. Experimental Procedure – Data Analysis

2.1 Experimental Setup

As a precursor to a full MED system, a single-effect distillation unit was constructed and tested. Since the input conditions to the single-effect are independently controlled, all operating conditions expected in any effect of a

full MED can be reproduced in the single stage. The key components of the experimental setup are illustrated in Fig. 4, and are the effect vessel, the multiphase heat exchanger, the final condenser, the vacuum pump and the peristaltic pumps for extracting brine and distillate product. In order to minimize thermal losses to the environment, the effect was thermally insulated.

The present implementation utilizes plate heat exchangers as a more compact and efficient way to transfer heat from the steam to the seawater, as opposed to the traditionally used shell-and-tube heat exchangers [20]. The steam will pass through the plates of the heat exchanger, condense, and return back to the boiler, while the saline water boils and thus evaporates. The water vapour is ported to the final condenser, in which it is cooled down by passing cold water through the heat exchanger and it condenses into the distillate product.

To ensure that the heat released from the heating steam will be transferred to the saline water, the condensation temperature of steam has to be higher than the boiling temperature of the saline water. To achieve this, the saline water boiling point is reduced by decreasing the pressure in the evaporator tank by a vacuum pump. The remaining brine water is removed from the evaporator tank continuously via a peristaltic pump.

Since low flow conditions were investigated, a critical challenge we had to face was the complete wetting of the heat exchanger plates, since it determines the heat transfer within the heat exchanger and thus the operational efficiency. During initial testing, it was observed that the plates were not all wetted; therefore a flow distributor was designed and tested in order to better distribute the seawater flow over the heat exchanger. Several distributor configurations were experimentally evaluated, and a configuration with 4 holes, each 3 mm in diameter and spaced 8.5 mm apart achieved the greatest wetting on the heat exchanger plates [21].

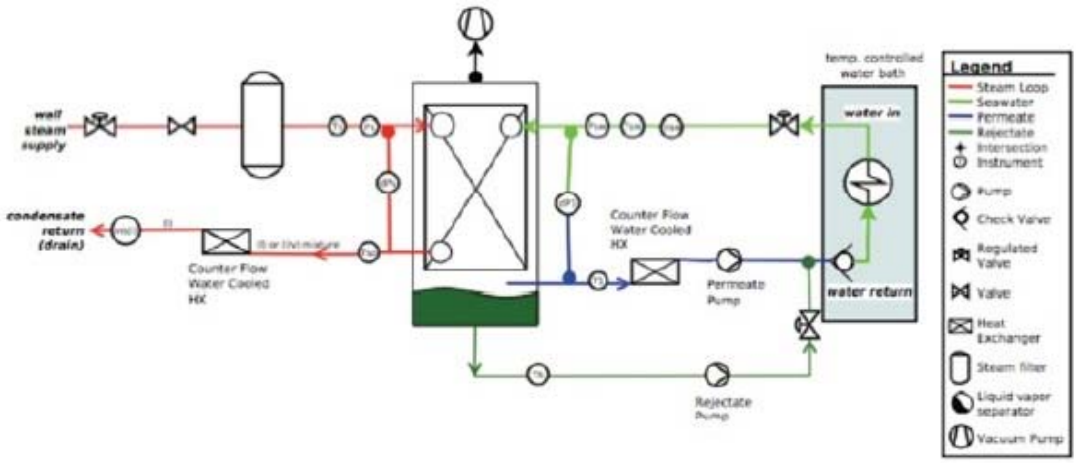

Fig. 4 Schematic of the singe effect distillation unit.

2.2 Data acquisition and analysis

The experimental process was as follows: Initially the effect was evacuated to remove all non-condensable gasses and then steam and seawater where allowed to flow. The startup process lasted about one hour, during which time the temperature of the system was gradually raised. Once a steady state was obtained, data acquisition commenced. A typical run lasted between 20-30 minutes, and consisted of recording effect temperature, pressure, flow-rates, and brine height level within the vessel. Temperatures were recorded using type-K thermocouples that were previously calibrated against a NIST traceable standard using an ice-point reference and an immersion heater, to reduce their error to ±0.4 °C in the 30-150 °C range. Subsequently, the parameter under investigation was varied and the process was repeated.

The aim during each run was to minimize the variation in flow properties and achieve a steady production of distillate. A statistical analysis was performed over all data samples gathered for a given run, and the variance and error were computed. The error bars correspond to an error propagation analysis. A 95% confidence interval was used reflecting a significance level of 0.05.

The steam generator employed had a cyclical variation in its output flowrate, attributed to its temperature controller. This lead to a fairly large variance in m_{st}, and thus large variances in all related quantities. Sample data from the flow-meters is presented in Fig. 5, where the variation in m_{st} can be clearly seen, whereas in contrast the seawater (m_{sw}) and brine (m_b) flow-rates are fairly steady. The fact that the steam flow rate variation does not affect the operation of the effect is an indication of the robustness of the MED process.

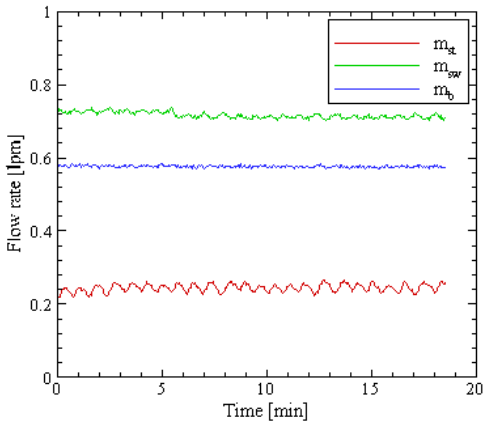

Fig. 5 Representative time record of flow meter sensor outputs collected from the single-effect MED

2.3 Test matrix

Measurements were made in order to characterize the performance of the single-effect distillation unit. The variation of the observed steam flow rate was taken into account in the data analysis. The steam generator was set at three different thermal power output levels ($Q_{e,1} < Q_{e,2} < Q_{e,3}$) and measurements were repeated for each input load. The device performance is measured by computing the performance ratio, *PR*, a metric for the efficiency of thermal distillation systems defined as the ratio between the distillate and steam flows fed to the evaporator. The range of parameters investigated is summarized in Table I.

Table I Range of parameters varied in experimental studies

Parameter	Units	Range
$Q_{e,1}$	[kW_{th}]	4.2 ± 0.2
$Q_{e,2}$	[kW_{th}]	5.7 ± 0.3
$Q_{e,3}$	[kW_{th}]	7.6 ± 0.4
m_{sw}	[lpm]	0.20 – 0.72
$T_{sw,1}$	[°C]	19 – 22
$T_{sw,2}$	[°C]	30 – 32

3. Experimental Results

The performance ratio obtained by varying the seawater flowrate for a given thermal input ($Q_{e,1}$) is presented in Fig. 6. The seawater flow rate is non-dimensionalized by the steam flowrate in order to aid comparison between the various cases of thermal input. The error bars represent the compounded uncertainty in the measurements due to each probes error. It is important to note that the line connecting the experimental points is a curve-fit meant to aid the reader in visualizing the data, therefore the maximum *PR* in the experimental points and the curve-fit might not be at exactly the same point. The same is true for the remaining figures of this text.

A maximum *PR* is observed for a normalized seawater flowrate of 2.5. When m_{sw} is decreased, there is not sufficient wetting of the heat exchanger plates, and so dry spots occur, leading to a decrease in the overall heat transfer coefficient, and hence a decrease in the performance of the device. On the other hand, m_{sw} is increased, a larger fraction of the available thermal energy is required for elevating the feed temperature to the boiling temperature, and so less energy is available for the phase change process, leading to less distillate production and a lower *PR*.

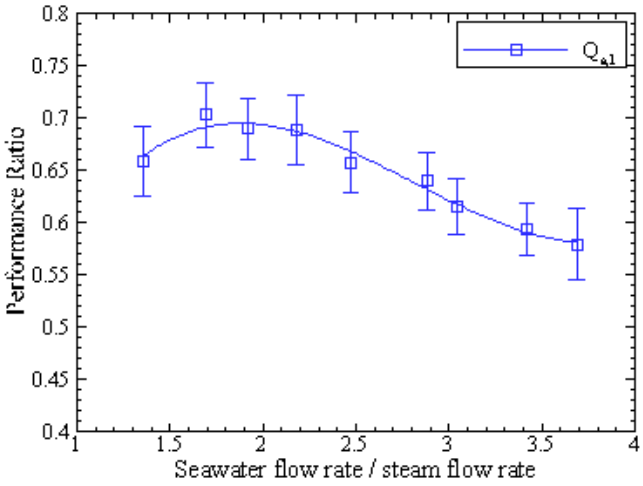

Fig. 6 Summary of results for single effect distillation for a constant heat input (T_{steam1})

The same trends as those observed in Fig. 6 for $T_{st,1}$ input conditions are present for all thermal input conditions, as summarized in Fig. 7. Here the error bars are omitted for clarity of the figure, but the magnitude of the error is similar to that presented in Fig. 6. For all thermal inputs, the maximum *PR* ratio measured remains almost constant at 0.71. Small variations in the magnitude of the *PR* are attributed to different seawater feed temperatures, as discussed below. As the thermal input to the system is increased, the maximum *PR* shifts to the left, e.g. to a lower seawater flowrate, as more thermal energy is available for the same quantity of seawater and thus evaporation and dry out will occur at lower flowrates.

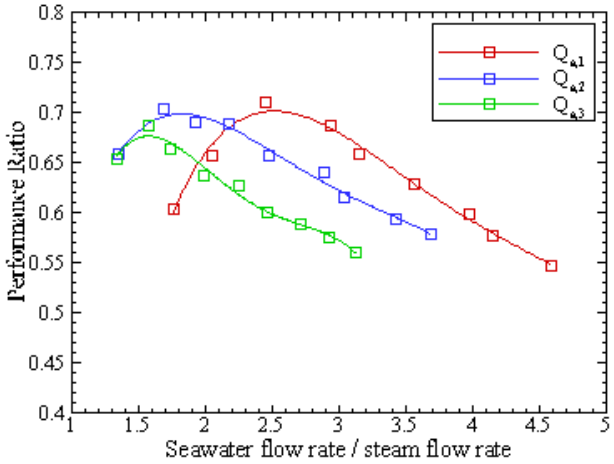

Fig. 7 Summary of results for single effect performance ratio for all three different heat input conditions ($Q_{e,1}$, $Q_{e,2}$ and $Q_{e,3}$)

Another parameter monitored was the temperature of the feed seawater. In a typical MED setup, the seawater would be preheated since it would be used as the cooling fluid in the final condenser. However, in the present setup, the seawater was not preheated and was drawn from a tank at ambient temperature. In order to outline the importance of the feed seawater temperature, the *PR* of the unit is given in Fig. 8 for the $Q_{e,2}$ thermal input condition, and for two different seawater feed temperatures. The seawater feed temperature mainly depended on the outdoor conditions and the season of the experiments. The experiments presented herein where performed at two different ambient conditions, nominally $T_{sw,1}$ = 21 °C and $T_{sw,2}$ = 31 °C. The shape of the two curves and the location of the maximum *PR* are similar. However, for $T_{sw,2} > T_{sw,1}$, higher *PR*'s are obtained, as, again, less thermal energy is required for the pre-heating of the seawater and thus more energy is available for the production of distillate.

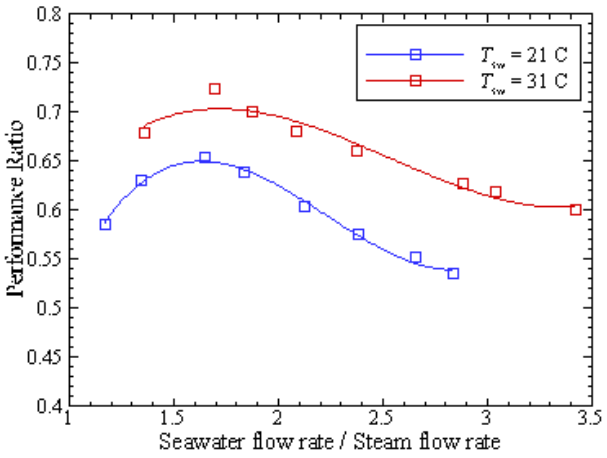

Fig. 8 The Performance ratio curve under different seawater feed temperatures for constant heat input load ($Q_{e,2}$)

4. Analysis of forward feed MED

A mathematical model for a single-effect distillation system is developed to analyze the system operating characteristics and the effect of various design parameters. The model is essentially a mass and energy balance, and follows similar models in the literature [22]. The major model assumptions are steady state operating conditions, zero salinity for the product water, and that no non-condensable gases are present in the system.

4.1 Mass balance equations

In the single effect distiller, the feed seawater ends up in the distillate and the brine. Therefore the conservation of mass and conservation of species equations can be written as:

$$m_{sw} = m_d + m_b \tag{1}$$

$$m_{sw}X_{sw} = m_bX_b \tag{2}$$

where m is the mass flow rate, X is the salinity, and the subscripts b, d, and sw denote the brine, distillate, and seawater.

4.2 Energy balance equations

In the evaporator, saturated steam that flows from the steam boiler at a rate of m_{st} is used to raise the temperature of the seawater from the initial temperature T_{sw} to the boiling temperature T_b. Additionally it supplies the latent heat required to evaporate the specified mass of vapour, m_d. Therefore, the evaporator energy balance is given as:

$$Q_e = m_{st}\lambda_{st} = m_{sw}C_p(T_b - T_{sw}) + m_d\lambda_v + Q_{loss,e} \tag{3}$$

where Q_e is the thermal load of the evaporator, C_p is the specific heat capacity at constant pressure of the brine, and λ is the latent heat of evaporation.

The condenser operates on the vapour formed in the evaporator, m_d. The latent heat of condensation is transferred to feed seawater with a mass flow rate of m_{sw} - m_{cw}. The feed seawater m_{sw} is introduced into the evaporator; while the remaining part m_{cw} which is known as the cooling water, is rejected. The vapour is assumed saturated at a temperature equal to T_v.

$$Q_c = m_d\lambda_v = (m_{sw} + m_{cw})C_p(T_{sw} - T_{cw}) + Q_{loss,c} \tag{4}$$

where Q_c is the thermal load of the condenser, and the subscripts cw, and v denote the cooling seawater, and condensing vapour.

Therefore, based on the equation given above, the overall energy balance for the system is:

$$m_{st}\lambda_{st} = m_bC_p(T_v - T_{sw}) + m_dC_p(T_d - T_{sw}) + m_d\lambda_v + Q_{loss} \tag{5}$$

where the vapour temperature T_b is then defined in terms of the boiling temperature T_b and the boiling point elevation (BPE)

$$T_b = T_v + BPE. \tag{6}$$

For the calculations of the thermophysical properties of seawater, standard correlations employed in the literature were used [23].

4.3 Heat exchanger model

The amount of heat to be transferred in the evaporator (Q_e) depends on the evaporator's surface area (A_e), the overall heat transfer coefficient (U_e) and the temperature difference of the steam T_{st} and the boiling temperature of the seawater T_{sw}.

$$Q_e = A_e U_e (T_{st} - T_b) \tag{7}$$

As it was mentioned above the Performance Ratio of the unit is defined as of the flow rates ratio of the distillate and the heating steam. Therefore the *PR* is given by:

$$PR = \frac{m_d}{m_{st}} = \lambda_{st} \Big/ \left[\lambda_v + C_p(T_v - T_{sw})\frac{X_b}{X_b - X_{sw}} + \frac{X_{sw}}{X_b - X_{sw}} C_p BPE\right] \tag{8}$$

4.4 Comparison with experimental data

The last step for the single effect characterization was the comparison of the experimental results with the theoretical results predicted by the control volume model described above, which is presented in Fig. 9. The theoretical curve was generated by feeding the model with the experimental steam flow rate, seawater flow rate and effect temperature (T_b), as well as the thermal input Q_e. The deviation of the theoretical curve from a linear curve is due to the error in the temperature measurement. As expected, the model captures the decreasing trend in *PR* experienced as the seawater flow rate increases. However, the simple one-dimensional model is unable to capture the dry out occurring at low flow conditions and thus is unable to predict the maximum in *PR*.

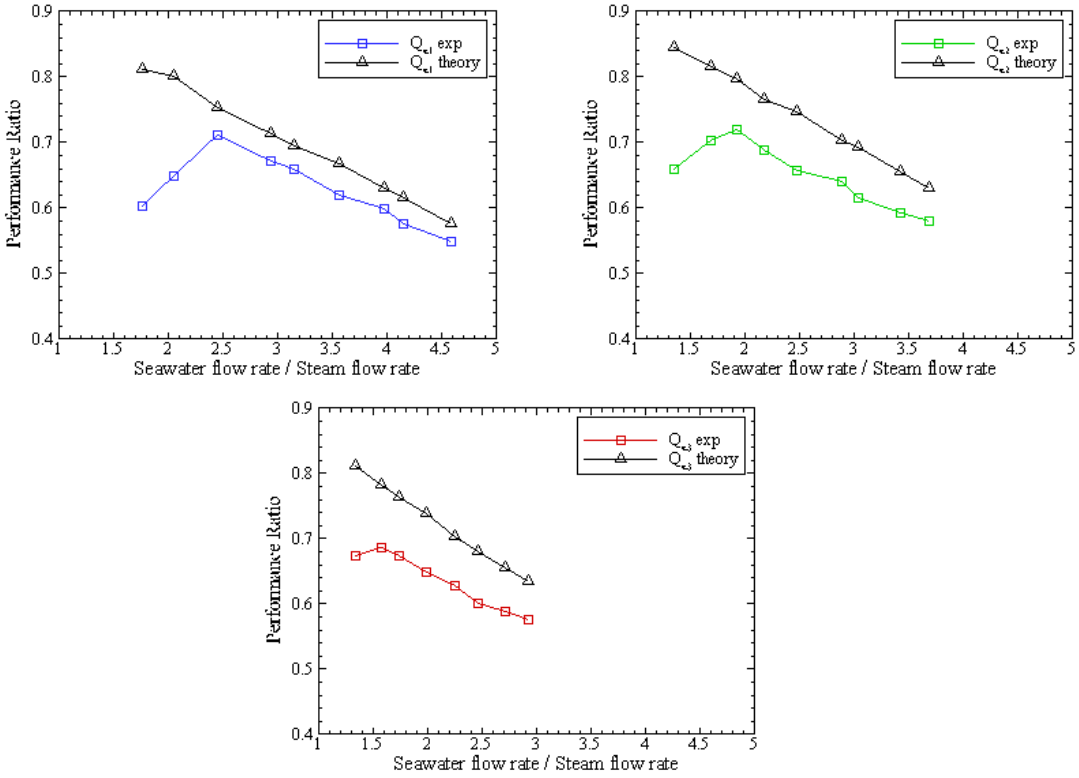

Fig. 9 Comparison of experimental results with the predictions from the ideal (Q_{loss} = 0) control volume model, for the three thermal input conditions.

5. Conclusions

Considering the existing water crisis that Cyprus is facing and the forecast for annual precipitation in the island, the need for development of new sustainable technologies such as seawater desalination is urgent. Furthermore the integration of a desalination unit with a concentrated solar power system gives the opportunity for cogeneration of electricity and heat, thus the energy needed for desalination can be obtained through a renewable energy source.

In this paper the experimental results of a single effect distillation unit were presented. The main conclusions from this work can be summarized as:

- A maximum performance ratio exists for each thermal input condition. This is where the single effect distillation unit performs the most efficiently, e.g. produces the maximum amount of distillate for a given amount of steam.
- Increasing the seawater reduces the amount of distillate produced; since more seawater mass is present and a larger fraction of the available thermal energy is devoted to sensible heating of the seawater.
- Decreasing the seawater reduces the amount of distillate produced; since less mass is available to completely wet the heat exchangers, dry spots occur reducing the overall heat transfer coefficient of the device and leading to a decrease in the amount of distillate produced.
- Increasing the temperature of the seawater feed increases the efficiency and the performance ratio of the device.
- The predictions of the one-dimensional theoretical model developed overall are satisfactory. The model is unable to capture the maximum in the performance ratio since it cannot capture the physics of the dry out on the heat exchanger plates.

Further to this study, a four effect distillation unit will be developed and evaluated in terms of the *PR*. Additionally the control volume model will be expanded into a multiple-effect model in order to compare with the experimental results.

Acknowledgements

The authors are grateful for funding from the STEP-EW project, which runs under the framework of cross-border cooperation programme “Greece-Cyprus 2007-2013” and is co-financed by 80% by the European Commission (European Regional Development Fund) and by 20% by national funds of Greece and Cyprus.

References

1. T. Zachariadis, Residential Water Scarcity in Cyprus: Impact of Climate Change and Policy Options, Water, 2 (2010), 788-814.
2. European, C., 2006. Water Scarcity and Droughts, Finland
3. T. Zachariadis, Climate Change in Cyprus: Impacts and Adaptation Policies. Cyp. Econ. Policy Rev., 6 (2012), 21-37.
4. 4 EC, 2007b. Water scarcity and droughts. Second interim report — June 2007. http://ec.europa. eu/environment/water/quantity/pdf/comm_ droughts/2nd_int_report.pdf. Accessed February 5 2014
5. IPCC, 2011. IPCC Special Report on Renewable Energy Sources and Climate Change Mitigation, Cambridge: Cambridge University Press.
6. P. Hadjinicolaou, C. Giannakopoulos, C. Zerefos, M.A. Lange, S. Pashiardis and J. Lelieveld, Mid-21st century climate and weather extremes in Cyprus as projected by six regional climate models, Reg. Env. Change 201 (2011), 441-457.
7. European Commission Green Paper on Adapting to Climate Change in Europe, Report, 2007.

8. M. Elimelech and W.A. Phillip, The Future of Seawater Desalination: Energy, Technology and the Environment, Science 333 (2011), 712-717

9. N.M. Wade, Distillation plant development and cost update, Desal, 136, pp. 3-12, 2001.

10. Vozar, M.D. Georgiou, M. Seong and J.G. Georgiadis, Analysis and Design of a Multi-Effect Desalination System with Thermal Vapor Compression and Harvested Heat Addition, Desal. Wat. Treat. 31 (2011), 339-346

11. M. Al-Shammiri and M.Safar, Multi-effect distillation plants: state of the art, Desal, 126, pp. 45-59, 1999.

12. M. Darwish, Feed water arrangements in multi-effect desalting system,Desal, 228, pp. 30-54, 2008.

13. S. Kalogirou, Economic analysis of a solar assisted desalination system, Ren. En., 12 (1997), 351-367.

14. J. Blanco, S. Malato, P. Fernandez-Ibanez, D. Alarcon, W. Gernjak and M. Maldonado. "Review of feasible solar energy applications to water processes." Ren. Sust. En. Rev., 13 (2009), 1437-1445.

15. A. Ghobeity, C.J. Noone, C.N. Papanicolas and A. Mitsos, Optimal time invariant operation of a power and water cogeneration solar-thermal plant, Sol. En. 85 (2011), 2295-2320.

16. The Cyprus Institute, “Solar Thermal Cogeneration of Electricity and Water”, ISBN 978-9963-2858-0-8, 2012.

17. P. Palenzuela, G. Zaragoza, D. Alarcon and J. Blanco, Simulation and evaluation of desalination units to parabolic-trough solar power plants in the Mediterranean region, Desal, 281, pp. 379-387, 2011.

18. L. Garcia-Rodriguez and C. Gomez-Camacho, Design parameter selection for a distillation system coupled to a solar parabolic through collector, Desal, 122, pp. 195-204, 1999.

19. Combined Solar Power and Desalination Plant: Techno-Economic Potential in Mediterranean Partner Countries, Report, 2010.

20. J.B. Tonner, S. Hinge, C. Legorreta, Plates – the next breakthrough in thermal desalination, Desal., 134 (2001) 205-211.

21. M.C. Georgiou, A.M. Bonanos, and J.G. Georgiadis, Evaluation of a Multiple-Effect Distillation Unit under Partial Load Operating Conditions. Conf. Pap. En., 2013 (2013), 482743.

22. H.T.El-Dessouky, and H.M.Ettouney. Fundamentals of Salt Water Desalination, Elsevier, 2002, pp. 20-44.

23. M.H. Sharqawy, J.H. Lienhard V and S.M. Zubair, Thermophyiscal porperties of seawater: a review of existing correlations and data, Desal. Wat. Treat. 16 (2010), 354-380.